The Earthquake Risk Model of Switzerland ERM-CH23

Athanasios N. Papadopoulos [1], Philippe Roth[1], Laurentiu Danciu[1], Paolo Bergamo[1], Francesco Panzera[1,5], Donat Fäh[1], Carlo Cauzzi[1], Blaise Duvernay[2], Alireza Khodaverdian[3], Pierino Lestuzzi[3], Ömer Odabaşi[4], Ettore Fagà[4], Paolo Bazzurro[4], Michèle Marti[1], Nadja Valenzuela[1], Irina Dallo[1], Nicolas Schmid[1], Philip Kästli[1], Florian Haslinger[1], Stefan Wiemer[1]

[1] Swiss Seismological Service (SED), ETH Zurich, Zurich, 8092, Switzerland
[2] Federal Office for the Environment (FOEN), Bern, Switzerland
[3] École Polytechnique Fédérale de Lausanne, Lausanne
[4] RED Risk Engineering + Development, Pavia, Italy
[5] Department of Biological, Geological and Environmental Sciences, University of Catania, Italy

Correspondence to: Athanasios N. Papadopoulos (th.papadopoulos@outlook.com)

Abstract. Understanding seismic risk at both the national and sub-national levels is essential for devising effective strategies and interventions aimed at its mitigation. The Earthquake Risk Model of Switzerland (ERM-CH23), released in early 2023, is the culmination of a multidisciplinary effort aiming to achieve, for the first time, a comprehensive assessment of the potential consequences of earthquakes on the Swiss building stock and population. Having been developed as a national model, ERM-CH23 relies on very high-resolution site-amplification and building exposure datasets, which distinguishes it from most regional models to-date. Several loss types are evaluated, ranging from structural/nonstructural and contents economic losses, to human losses, such as deaths, injuries and displaced population. In this paper, we offer a snapshot of ERM-CH23, summarize key details on the development of its components, highlight important results and provide comparisons with other models.

1 Introduction

Natural hazards can cause widespread damage, loss of life, and disruption to critical services such as water, power, and transportation. Earthquake risk mitigation programs are effective, and as cities and populations continue to expand, they become increasingly vital to safeguard lives, infrastructure, and economic stability. A study from the National Institute of Building Sciences in the US estimated that Federal Mitigation Grants for earthquake hazards save 3 dollars per 1 dollar spent (National Institute of Building Sciences, 2019). –Catastrophe risk models, in particular, can aid governments and other stakeholders in determining the potential impact of different perils, identifying high-risk areas, and prioritizing resources and investments for preparedness and mitigation. They can further inform emergency response plans, helping increase the resilience of communities to catastrophic events. As such, the development and operation of national catastrophe risk models and related byproducts is increasingly seen as the basis for designing an effective data-driven disaster risk reduction strategy. Strong earthquakes in particular, compared to other natural hazards, are characterized by rather infrequent occurrence and high potential for causing significant devastation. This low-probability-high-consequence feature of seismic risk hinders societal

preparedness, as both public interest and actionable data are missing. In contrast, it makes modelling efforts all the more important for anticipating future scenarios and drawing mitigation actions. The latter could involve reduction (e.g., retrofit of existing structures, update of design codes for new construction, educational campaigns), transfer (e.g., insurance) or planned retention (e.g., dedicated disaster funds) of the risk.

Seismic risk modelling initiatives at the national level have been undertaken to varying extents in different countries, such as Italy (Dolce et al., 2021), USA (FEMA, 2010; Jaiswal et al., 2015), Canada (Hobbs et al., 2023), Germany (Tyagunov et al., 2006), Spain (Salgado-Gálvez et al., 2015), and Portugal (Marques et al., 2018). There have also been attempts to model risk at continental or global scales. In Europe, an open earthquake risk model (ESRM20; Crowley et al., 2021) has been released as an output of the European Union's Horizon 2020 SERA project (www.sera-eu.org). ESRM20 is a uniform risk model that covers 45 European countries and is the result of a concerted effort among the research community in Europe. Lastly, global models have also been compiled, such as the UNISDR's Global Assessment Report (GAR; Cardona et al., 2014), and most notably, the 2018 Global Seismic Risk Map (Silva et al., 2020b) developed by the Global Earthquake Model (GEM) Foundation. The latter has allowed access to a uniform view of risk across the globe, a valuable resource, particularly for previously under-studied regions.

In Switzerland, the Federal Council commissioned in 2013 the Federal Office for the Environment (FOEN), in cooperation with the Swiss Seismological Service (SED) and the Federal Office for Civil Protection (FOCP), to prepare a feasibility study and project plan to develop a national earthquake risk model. Based on these documents, the Federal Council commissioned in 2017 the SED, in cooperation with FOEN and FOCP, to develop this model until 2023. In the following sections, we give an overview of ERM-CH23 and its subcomponents (seismic source, ground motion, site amplification, fragility, consequence and exposure models) and then present primary results and insights such as comparison with other published models.

2 Seismicity in Switzerland

In Switzerland, earthquakes are considered to be the natural hazard with the potential for causing the greatest damage. The 2020 Risk Report (FOCP, 2020), published by the FOCP, ranked earthquakes as the third largest risk faced by Switzerland, after electricity shortages and pandemics. Overall, the seismicity in the country is considered moderate with three to four earthquakes a day recorded on average within the country and around its borders by the monitoring network of the Swiss Seismological Service (SED; www.seismo.ethz.ch), the federal agency responsible for monitoring earthquakes in Switzerland and its neighbouring regions Overall, the seismicity in the country is considered moderate with three to four earthquakes a day recorded on average within the country and around its borders by the Swiss Seismological Service (SED) at ETH Zurich. A destructive earthquake with moment magnitude (M_w) of 6.0 or above can be expected to occur on average every 50 to 150 years (Wiemer et al., 2016). The most seismically active regions are found in the Valais and Graubünden cantons, as well as the southern Rhine Graben, a rift system located in the northeastern part of the country. The 1356 Basel earthquake is the largest known to-date earthquake to have struck Switzerland, with an estimated moment magnitude of 6.6. It caused widespread

65   damage (Fäh et al., 2009) throughout Switzerland and neighbouring countries, and was felt as far away as Paris. Other notable historical events in the last 200 years include the 1855 M_w 6.2 Visp earthquake (Fritsche et al., 2006) and the 1946 M_w 5.8 Sierre earthquake (Fritsche and Fäh, 2009). Figure 1~~Figure 1~~ shows the spatial and temporal pattern of known earthquakes of magnitude above 5.0 in Switzerland.
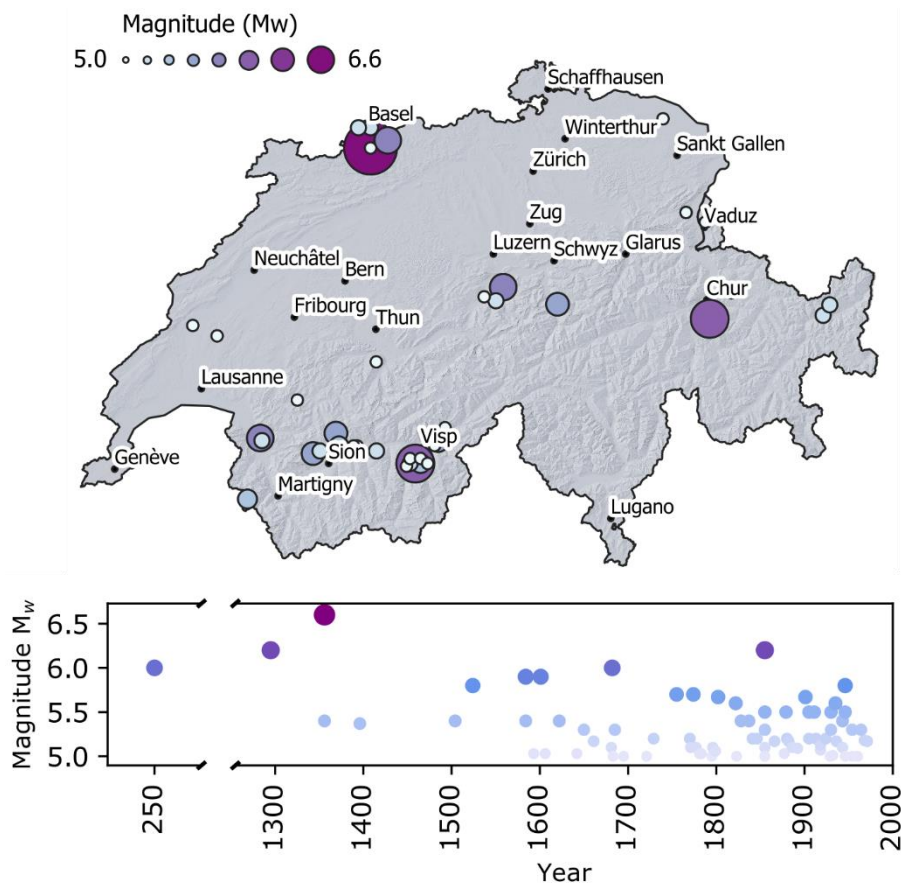
Figure 1. Locations, dates and size of known historical earthquakes with magnitude M_w>5.0 in Switzerland (ECOS-09 catalogue;
70   **Fäh et al., 2011)**

3 The Earthquake Risk Model of Switzerland (ERM-CH23)

3.1 Seismic hazard

ERM-CH23 primarily relies on the 2015 Seismic Hazard Model (SUIhaz2015; Wiemer et al., 2016), which is the authoritative national seismic hazard model of Switzerland. While SUIhaz2015 serves as the basis, a number of adjustments were made to
75   tailor it for use within the context of ERM-CH23 and are succinctly detailed in the sections to follow, and in Wiemer et al. (2023) in more detail.

3.1.1 Source model

The seismogenic source model of SUIhaz2015 results from a weighted ensemble of four individual source models. The latter include an area source model (SEIS-15) and a smoothed seismicity model (CH14), developed specifically for SUIhaz2015. The other two models are sourced from past seismic hazard models, i.e. SEIS04 (Wiemer et al., 2009) and ESHM13 (SHARE Project; Woessner et al., 2015). From the ensemble earthquake rate model, the activity rates corresponding to the 2.5%, 16%, 50%, 84%, 97.5% quantiles were obtained and assigned as five alternative logic tree branches with weights corresponding to the associated area under a normal distribution that they represent. For further details on the source model of SUIhaz2015, the reader is referred to Wiemer et al. (2016).

In ERM-CH23, the five original logic tree branches are "collapsed" into a single branch with weighted average rates. The motivation behind this choice was 1) to reduce the significant computational cost associated with risk analyses, and 2) also to avoid the synchronous assignment of improbable rates in all sources (e.g. in the 2.5th or 97.5th quantile rate branches) across the country. The bias from the latter would invalidate any estimation of epistemic quantiles (although an argument exists that it could be advantageous for the evaluation of mean estimates). Similar reasoning for using a single collapsed branch has been made in other models (e.g. Crowley et al., 2021).

The maximum magnitude is spatially variable and in the range of M_w 6.5 to 7.3 (Wiemer et al., 2016). The minimum magnitude, originally set to M_w 4.0 in SUIhaz2015, was increased to M_w 4.5 for ERM-CH23, on the basis that smaller events are not of particular engineering significance (Bommer and Crowley, 2017).

3.1.2 Ground shaking

ERM-CH23 is built upon two main sub-models, one that uses spectral acceleration, henceforth referred to as SAM and given a weight of 0.7 in the overall logic tree (Figure 6), and one that uses EMS-98 (Grünthal, 1998) macroseismic intensity, henceforth referred to as MIM and given a weight of 0.3. The ground shaking in SAM is modelled with the same set of ground motion models (GMMs) used in SUIhaz2015 (Wiemer et al., 2016; Edwards et al., 2016). These include empirical models based on datasets in Europe and worldwide, such as those of Zhao (2006) Chiou and Youngs (2008), Cauzzi and Faccioli (2008), and Akkar and Bommer (2010), adjusted to match the amplification and attenuation levels typical of the Swiss reference rock (Edwards et al., 2016; Wiemer et al., 2016; Poggi et al., 2011). They also include the Swiss-specific stochastic models of Edwards and Fäh (2013) and Cauzzi et al. (2015), obtained by simulating ground shaking for various source, path and site-specific parameterizations. Different GMMs and weights are set for each of four identified tectonic regimes, namely Alpine Shallow, Alpine Deep, Foreland Shallow, Foreland Deep. Each tectonic regime represents a different branching set in the logic tree, with 18, 16, 18 and 16 GMMs, respectively. The total number of GMM logic tree branch combinations reaches 82,944 (18 x 16 x 18 x 16). The full GMM logic tree is reported in the electronic supplement. Further details on the selection, weighting, and statistical performance of these models in Switzerland can been sought in Edwards et al. (2016).

For what concerns MIM, a selection of intensity prediction equations (IPEs) was carried out for ERM-CH23. A residual analysis was conducted on the macroseismic dataset for the region, in order to compare a collection of candidate IPEs. The
110 latter were ranked and four of the~~m~~ best performing ones~~(Table 1)~~ were then selected (Table 1) to represent the body, center and range of intensity data. Besides the residual analysis, considerations were made to compile a set that encompasses different epistemic views (e.g. amplitude and attenuation trends) with members calibrated on different datasets (the two ECOS-09 models are fit on Swiss macroseismic observations, whereas the other two on wider datasets).~~.~~

115 **Table 1. Intensity prediction equations used in ERM-CH23**

Name	Weight	Reference
ECOS09variableDepth	0.2	(Fäh et al., 2011)
ECOS09fixedDepth	0.3	(Fäh et al., 2011)
BaumontEtAl2018High2210IAVGDC30n7	0.3	(Baumont et al., 2018)
Bindi2011RHypo (with conversion to moment magnitude M_w)	0.2	(Bindi et al., 2011)

Finally, some adjustments were carried out in the aleatory uncertainty modelling of the IPEs and GMMs. For the former, it was decided to use the intra- and inter-event sigma of the Baumont et al. (2018) model, since the other functions do not distinguish into intra- and inter-event components, which is important for risk analyses. On the GMM side, the inter-event
120 sigma of the original functions is maintained, while the intra-event sigma is modelled as site-specific and derived together with the site amplification model (see following section) to ensure compatibility.

3.1.3 Site amplification

As a component of ERM-CH23, a new ground motion site amplification model was developed (Bergamo et al., ~~under review~~2023; Wiemer et al., 2023), covering the entire Switzerland in a homogeneous manner. This model is based on two
125 datasets. The first one comprises site amplification factors that were measured at seismic stations across Switzerland, while the second one is composed of site condition indicators that are known to be correlated with local seismic response. The empirical spectral modeling technique (ESM; Edwards et al., 2013), was used to compute Fourier amplification functions at instrumented sites, using earthquake recordings from 2000 to 2021; the amplification was then translated from the Fourier to the pseudo-spectral acceleration (Sa) domain resorting to random vibration theory (Liu and Pezeshk, 1999). The selected site
130 condition indicators~~,~~ (~~ including the ~~lithological classification of Switzerland, multiscale topographic slope, and depth-to-bedrock)~~,~~ were combined with the empirical amplification factors using the regression-kriging algorithm (Hengl et al., 2007). To allow coherent integration of the ground motion and site amplification modules, corresponding maps of the site-to-site variability (φ_{S2S}) and the single-site within-event variability (φ_{SS}) were also produced and used to define the overall intra-event variability. The latter site-specific estimate was used to replace the intra-event uncertainty term of the employed GMMs. The

135   site model is derived for four intensity measures, namely the geometric mean (of the two horizontal components) Peak Ground Velocity (PGV) and pseudo-spectral acceleration at 3 periods (0.3 s, 0.6 s and 1.0 s). The Sa(0.3 s) and Sa(0.6 s) models are employed in SAM, whereas the site amplification maps for PGV, Sa(0.3 s) and Sa(1.0 s) were further translated into macroseismic intensity aggravation layers (e.g. Figure 2Figure 2) for use with the IPEs and associated macroseismic intensity-based vulnerability functions. The conversion to macroseismic intensity aggravation was performed using the Faenza &

140   Michelini (2011, 2010) relations and the correction factors estimated by Panzera et al. (2021), the latter to take into account the shift from the reference soil condition of the GMMs to that of the IPEs.
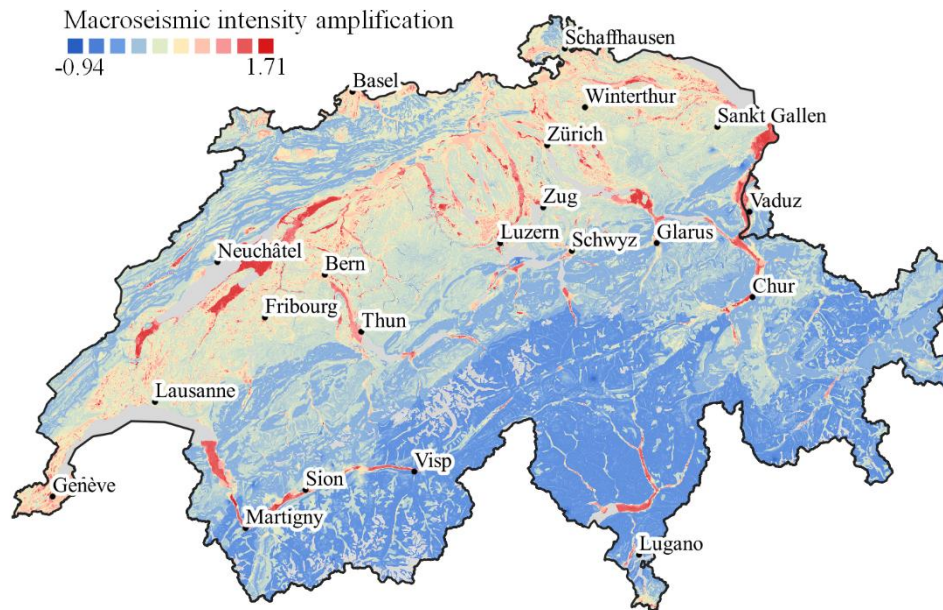
Figure 2. Example of macroseismic intensity aggravation map, derived from a Sa(0.3 s) proxy.

3.2 Seismic vulnerability

145   **3.2.1 Taxonomy**

According to several surveys carried out in Switzerland (e.g. Lestuzzi et al., 2016), the building taxonomy proposed in Lagomarsino and Giovinazzi (2006) is suitable for application to Switzerland with minor modifications (Table 2).

Table 2. ERM-CH23 building taxonomy

Typology	Description		Height	Typology	Description	Height
M1_L	Unreinforced	masonry	≤ 3 stories	S	Steel	any
M1_M	(Dry stone)		4 – 6 stories	T	Timber	any
M3_L			≤ 3 stories	M6_L		≤ 3 stories

M3_M	Unreinforced masonry (Rubble stone)	4 – 6 stories	M6_M	Unreinforced masonry – RC floors	4 – 6 stories
M3_H		≥ 7 stories	M6_H		≥ 7 stories
M4_L	Unreinforced masonry (Dressed stone)	≤ 3 stories	RCmix_L	Mixed shear wall and RC frame	≤ 3 stories
M4_M		4 – 6 stories	RCmix_M		4 – 6 stories
M4_H		≥ 7 stories	RCmix_H		≥ 7 stories
M5_L	Unreinforced masonry (old bricks)	≤ 3 stories	RCW_L	Shear wall	≤ 3 stories
M5_M		4 – 6 stories	RCW_M		4 – 6 stories
M5_H		≥ 7 stories	RCW_H		≥ 7 stories
Ind	Industrial type	any			

3.2.2 Fragility functions

Two different sets of fragility curves were derived, one in terms of macroseismic intensity for the MIM logic tree branches of the overall model and one in terms of spectral acceleration (at 0.3s or 0.6s) for the SAM branches (Wiemer et al., 2023). The MIM fragility model relies on the methodology described in Lagomarsino and Giovinazzi (2006), Lagomarsino et al. (2021), and Bernardini et al. (2010), together with engineering judgment about Swiss practice.

For the development of the SAM fragility functions, a statistical investigation of building blueprints was first exploited to identify average geometric characteristics of various building types. Capacity curves, idealized in bilinear form, were then obtained from numerical models (Lestuzzi et al., 2017). For most typologies 1000 capacity curves were then generated using the statistical model, covering material uncertainties. The method detailed in Michel et al. (2018) was followed to derive analytical fragility curves in terms of EMS-98 (Grünthal, 1998) damage states ranging from slight damage to collapse. Further details on the definition of capacity curves and the methodology followed to derive fragility curves can be found in (Wiemer et al., 2023).

3.2.3 Consequence model

A consequence model that relates damage to loss has been compiled for application to Switzerland (Wiemer et al., 2023). Different approaches were used for each of the five loss types of interest, depending on the availability of data. In brief, injuries and deaths were modelled based on the estimates given by HAZUS (FEMA, 2010), NCPD (2018), and Spence et al. (2007). Estimates of displaced population were instead adopted from the empirical data harmonized by the Italian National Civil Protection Department (NCPD, 2018). Displaced population in ERM-CH23 refers to households that have been displaced either in the short- or long-term. Content damage-to-loss estimates have also been adopted from the literature, and more precisely from HAZUS (FEMA, 2010).

On the other hand, the structural/nonstructural damage-to-loss functions have been derived analytically adopting the loss estimation methodology of FEMA P-58 (FEMA, 2018). For each building typology, the prescriptive damage states as per the

EMS-98 scale were matched to associated structural demand thresholds sourced from the literature (Wiemer et al., 2023). Archetype blueprints were used to infer quantities and features of structural elements such as load-bearing masonry walls, spandrels and slabs. The quantity estimator tool of FEMA P-58 was also used to determine the non-structural component quantities with uncertainty. Fragility and consequence functions for damageable structural and non-structural components, present in Swiss buildings, that were not available in FEMA P-58, were gathered and collated from other sources (Mouyiannou et al., 2014; Ottonelli et al., 2020; Rossi et al., 2021; Cardone, 2016; Cardone and Perrone, 2015; Magenes and Calvi, 1997; Avila et al., 2012). The repair and replacement costs were adjusted using a macro-economic model in view of the construction dynamics between the reference country (from which cost functions were available, i.e. Italy or the US) and Switzerland.

The repair cost conversion factor ($RCCF$) to be multiplied with the original (reference country) cost estimates was obtained as per Equation (1), building upon previous suggestions by Porter et al. (2015), Papadopoulos et al.(2019) and Silva et al. (2020a):

$$RCCF = (r_{lab} \cdot f_{lab} / r_{prod}) + (r_{mat} \cdot f_{mat}) + r_{m\&p} \cdot f_{m\&p} \qquad (1)$$

Here, f_{lab}, f_{mat} and $f_{m\&p}$ represent the proportion of the total repair cost associated with labour, materials, and margins and preliminaries, respectively, in the reference country (from which the cost is being adapted). On the other hand, r_{lab}, r_{mat} and $r_{m\&p}$ denote estimated ratios of the costs of labour, material, and margins and preliminaries between Switzerland (numerator) and the reference country (denominator). These parameters were determined following an extensive survey of both national and international sources, including the statistics bureaus of Italy, Switzerland and the United States, as well as Turner and Townsend (2019), ARCADIS (2019), Comune di Milano and Regione Lombardia (2021), and Raetz et al. (2020). Equation (1) also requires the difference in labour productivity between the target and reference countries $r_{prod} = c_{prod}^{target} / c_{prod}^{reference}$.

where c_{prod} represents labour productivity and is computed as:

$$c_{prod} = \frac{GVA}{\# \text{ of persons employed} \times \text{average workers compensation}} \qquad (2)$$

where GVA denotes the Gross Value Added to the construction sector, while the denominator is the product of the number of persons employed in the construction sector multiplied by the hourly associated worker compensation. Simply put, it represents value added per dollar spent on labour. These inputs were collected from the public databases of EUROSTAT, the OECD and the Federal Statistical Office of Switzerland. Table 3 report the inputs to Equation (1) that were used, while the resulting conversion factors were obtained equal to 1.4 for adjusting US cost data, and 2.73 for adjusting Italian cost data.

Table 3. Cost conversion function input parameters

	r_{lab}	r_{mat}	$r_{m\&p}$	f_{lab}	f_{mat}	$f_{m\&p}$	r_{prod}
USA-to-CH	0.81	1.65	1.06	0.425	0.40	0.175	0.66
ITA-to-CH	2.06	2.22	1.52	0.35	0.545	0.105	0.52

200 Adjustments were also made to account for inflation (e.g. the FEMA P-58 were representative of prices in 2012). Furthermore, technical/professional fees that arise on top of the operational costs of repairs are not accounted for in FEMA P-58. Previous research has shown that they can constitute up to 14% of the operational expenses (Di Ludovico et al., 2017a, b). As such, the percentage cost of technical fees added on top of our estimated repair costs was determined as 5% for DS1 and DS2, and 13% for the rest, in recognition of relevant national data on such fees reported in ETH Zurich (2015). Further details on the
205 development of the consequence model can be found in Wiemer et al. (2023).

3.2.4 Vulnerability functions

Vulnerability functions were derived by combination of the fragility and consequence models. Figure 3 shows a comparison of the structural/nonstructural vulnerability curves for the four most prevalent typologies in Switzerland (see Figure 5). As expected, the pure masonry typologies (M3, M5) are more vulnerable, with damage onset expected from rather low intensity
210 levels. The reinforced concrete wall (RCW) buildings, as well as the M6 typology which combines concrete and masonry elements are thought to be less vulnerable with damage expected at higher intensity values.
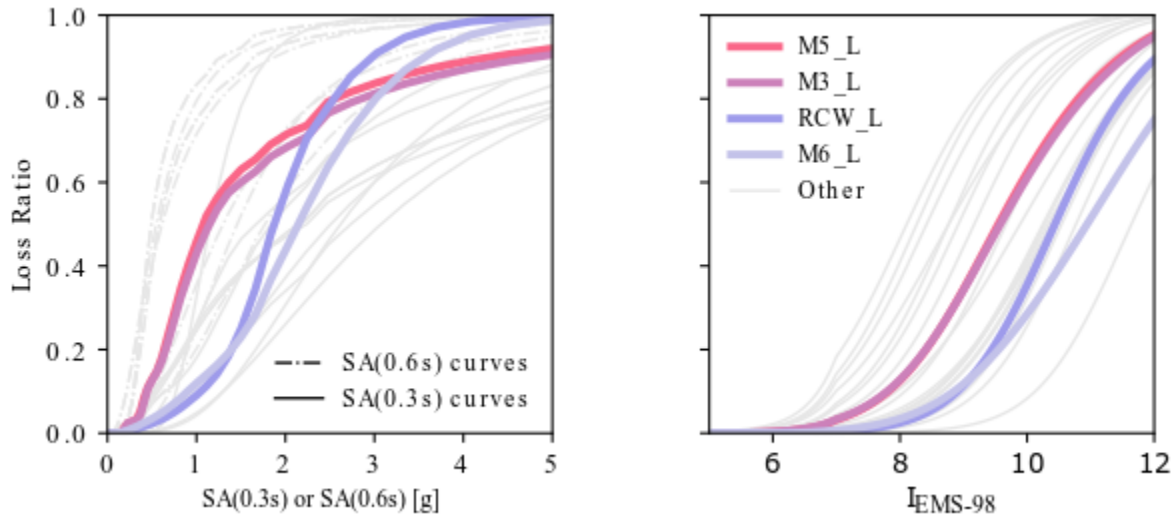
Figure 3. SAM (left) and MIM (right) structural/nonstructural vulnerability curves

3.3 Building exposure

215 The exposure model describes the location, value, occupants and typological characteristics of the buildings at risk. At the base of the ERM-CH23 exposure model lies an extensive geo-referenced database of all building objects in Switzerland, assembled by the Federal Office for the Environment (FOEN). Further details on the building database can be found in FOEN (2021) and Hügli et al. (2021), as well as in Wiemer et al. (2023). ERM-CH23 makes use of over 2.25 million building entries

in the database, after excluding close to 900'000 objects with an unclassified function or a volume above ground smaller than 200 m^3 (typically bungalows, storage sheds, bus shelters, etc).

Among others, the building database includes information such as the period of construction, building function, footprint area, volume and height (which is then used to define the number of stories) as obtained from digital surface and digital terrain elevation models. The reconstruction (replacement) cost is determined for each building according to Röthlisberger et al. (2018), using the building volume, the building function and the building zone category as predictor variables. The replacement value of building contents is computed as a fraction of the building reconstruction value, and varies from 0.19 to 0.65 depending on the building function. The modelled values were further validated using data from the cantonal building insurance companies. The number of occupants in each building is defined through de-aggregation of geo-referenced housing and employment statistics. For the estimation of human losses, ERM-CH23 uses a static (time-agnostic) equivalent number of occupants in each building that is obtained as a weighted average of residents, employees, students (in school buildings) and patients (in hospitals), as well as allowing for a share of the population being outdoors at the time of the earthquake. For further details the reader is referred to Wiemer et al. (2023).

Most of the exposure is concentrated at the Swiss plateau, north of the Alps (Figure 4a), especially around urban centres, such as Zurich, Geneva, Basel and Bern. The vast majority of the Swiss building stock consists of low-rise buildings of 1 to 3 stories (Figure 4b). High-rise buildings (>7 stories) are quite rare and concentrated in the major urban centres, such as Geneva, Zurich and Basel. Figure 4d shows the distribution of buildings constructed in different time periods. It appears that only a small fraction of the total was built after the introduction of seismic codes in 2003, with a significant amount of construction having taken place within the 1971-1990, 1946-1970 and <1919 periods. The total value of the modelled building stock and contents amounts to 2.9 trillion CHF and 0.8 trillion CHF, respectively. About 70% (structural/nonstructural) and 54% (contents) of this value comes from residential buildings. Commercial and public buildings add up to about 18% and 23% of the total structural/nonstructural and content values, while industrial buildings add up to about 10% and 20%, respectively. Agricultural buildings make up about 3% of the total value. The share of buildings of different occupancy by canton is illustrated in Figure 4c.
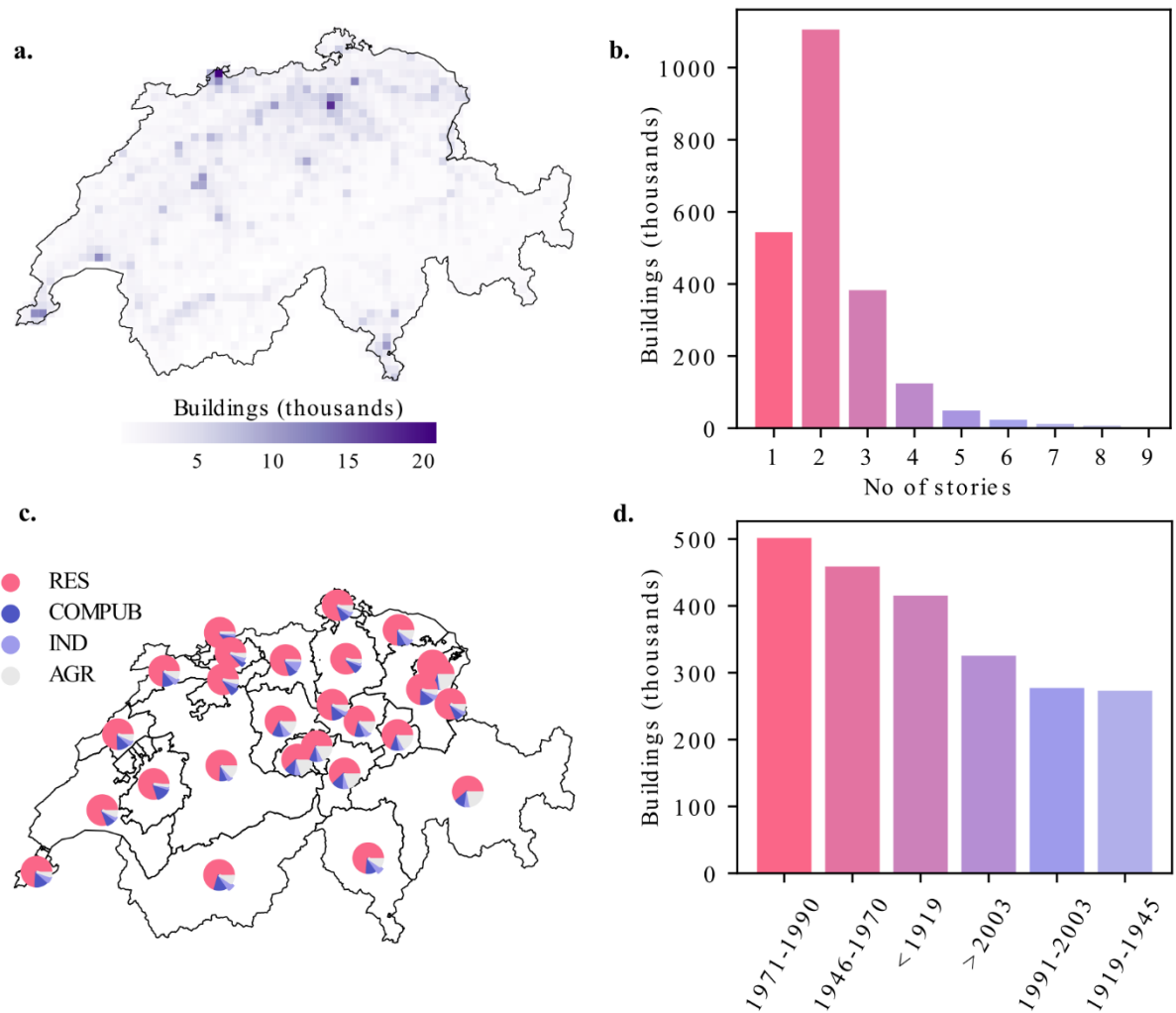
Figure 4. (a) Spatial distribution of buildings across Switzerland, (b) distribution of buildings by number of stories, (c) cantonal distributions of buildings by occupancy, (d) distribution of buildings by construction period.

The prevalence of different structural typologies in the Swiss building stock was assessed by means of field surveys carried out in the cities of Basel, Solothurn, Sion, Yverdon-les-Bains, Neuchâtel and Martigny (e.g. see Diana et al., 2019). Subsets of the building stock at these locations were visually assessed and assigned to a structural typology as per the taxonomy given in Table 2. The survey outcomes were used in two alternative ways within ERM-CH23 (Wiemer et al., 2023). In the first one, the statistics of structural systems were obtained, conditional on two attributes: the construction period and the height of the building (1-3 stories, 4-6 stories, >7 stories). Subsequently, a structural typology was assigned to each database entry by random sampling from the aforementioned conditional statistics. The second approach involved training a random forest algorithm (Tin Kam Ho, 1998) on the attributes of the database matched to the results of the field surveys. The random forest algorithm was then executed to predict the typologies of the remaining database entries. The two approaches constitute two

255 alternative logic tree branches of the ERM-CH23 framework. The rate-based (RB) approach was given a weight of 0.25 and the random forest (RF) based procedure was given a weight of 0.75. Figure 5 shows the share of the main typologies in Switzerland, as well as in the large municipalities of the main urban centers and in the smaller municipalities comprising the rest of the country. In general, masonry is the predominant construction material, with M3 (unreinforced rubble stone masonry), M5 (unreinforced old brick masonry), and M6 (unreinforced masonry with RC floors) being the most common. Reinforced

260 concrete wall (RCW) buildings also make up a significant, albeit lower, fraction of the building stock.
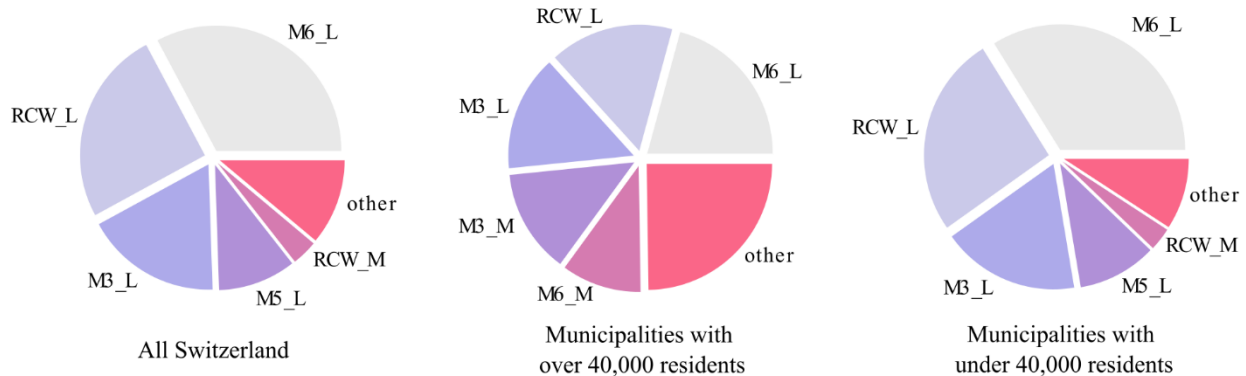
Figure 5. Share of different building typologies in the entire Swiss building stock (left), in large municipalities (middle), and in small municipalities (right)

265 Since the ERM-CH23 exposure numbered more than 2 million individual buildings, it had to be aggregated on a spatial grid to facilitate the risk computation. After investigating different options (Wiemer et al., 2023, Papadopoulos et al., ~~in preparation~~2024), the aggregation was performed on a 2 km x 2 km regular grid, along with some further considerations for minimizing any resulting errors. More precisely, the site parameters at the locations of buildings within each cells were first clustered with the K-means (MacQueen, 1967) approach. Buildings (of the same typology and postal code) belonging to each

270 of five (SAM) or three (MIM) grid cell clusters were placed in adjacent locations near the cell centroid and merged into one macro-asset. At each cluster location, the associated cluster centroid site parameters were assigned. Moreover, the merging of buildings into macro-assets (i.e., single assets with replacement values equal to the sum of the values of the buildings being aggregated), implies a perfect correlation of the ground motion and loss residuals (given ground motion) across the buildings being aggregated. To remove the effect of this implicit correlation of the loss ratios, vulnerability curves for macro-assets of n

275 buildings (where n was taken equal to 1, 5, 20, and 85) were estimated and used for macro-assets of different sizes. This was done by sampling the single building loss ratio multiple times for each of the n buildings comprising it, summing up to get the total macro-asset loss, and then building the updated loss ratio distribution given each ground motion level (Wiemer et al., 2023, Papadopoulos et al., ~~in preparation~~2024).

3.4 Modelling of uncertainty

280 Undoubtedly, there are large uncertainties involved in earthquake risk modelling. As usual, aleatory uncertainties are considered in the modelling of earthquake occurrence (~~via a~~modelled as a Poisson process), in the modelling of ground motion (modelled with a lognormal distribution for ground motion or a normal distribution for intensity), as well as in the modelling of loss given ground motion (modelled with a beta distribution). Epistemic uncertainties in ERM-CH23 are captured via a logic tree approach, as already alluded earlier on. Figure 6 illustrates the logic tree set up that was adopted. A primary branching

285 distinguishes the MIM and SAM sub-models, with further branching levels for ground shaking modelling, site amplification and building mapping. The logic tree numbers 24 MIM-specific end-to-end branches and 165,888 SAM-specific end-to-end branches. For the risk calculations, all MIM branches were considered, whereas 400 SAM branches were randomly (based on their weights) selected and analysed.
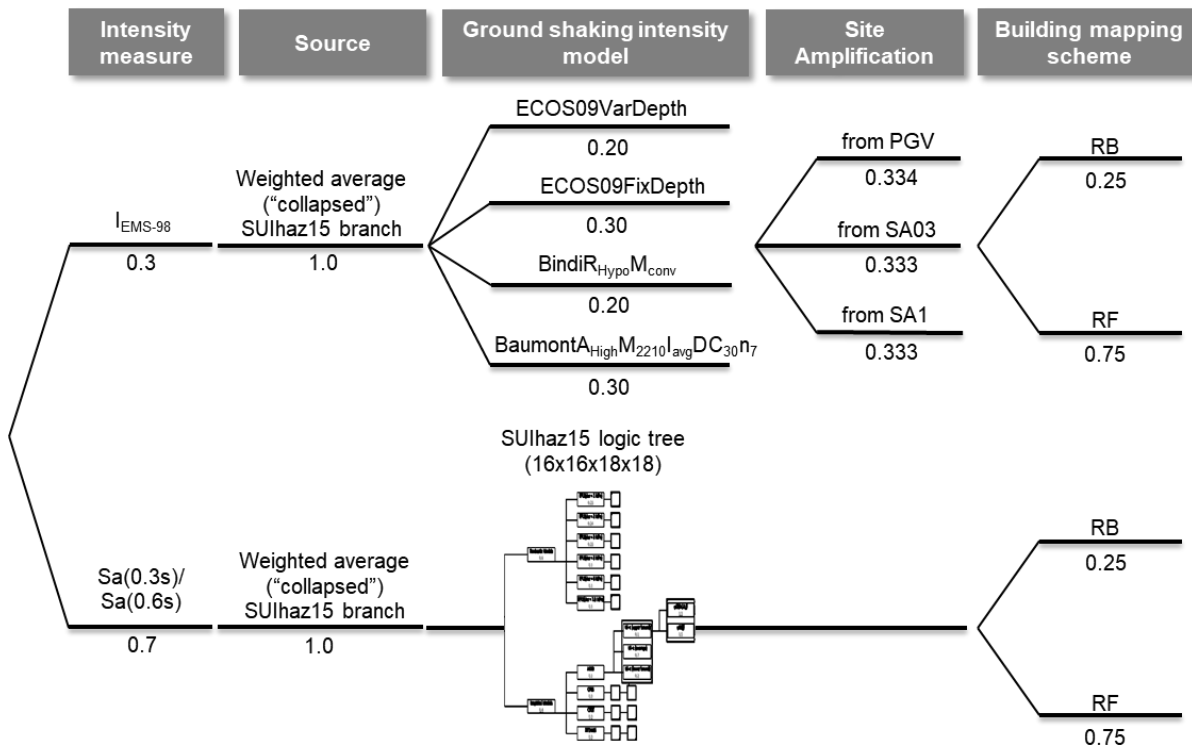
290 **Figure 6. The logic tree of ERM-CH23**

4 Earthquake risk assessment

To assess the earthquake risk over a spatially distributed exposure, a so-called event-based approach is required that starts with the generation of stochastic earthquake catalogues. ~~based on Monte Carlo simulations is typically required.~~ Usually, this is followed by the simulation of ~~An event-based probabilistic earthquake risk assessment starts with the generation of a large~~

number of stochastic earthquake catalogues and the generation of associated random ground motion fields for each generate earthquake rupture in the catalogue. The simulated ground motion intensity values at each site are then passed onto the vulnerability functions associated with the building typologies at each site. The asset-specific losses are then sampled and added to compute the total loss for the given earthquake. Finally, the sample of loss estimates is then used to obtain standard risk metrics, such as average annual losses (AAL) and probable maximum loss (PML; herein defined as loss versus return period of exceedance) curves.

All calculations are carried out using the open-source OpenQuake engine v3.14 (Pagani et al., 2014) developed by the GEM foundation. For each of the 24 MIM logic tree branches, 20,000 1-year long stochastic earthquake catalogues were generated, while 10,000 1-year long catalogues were simulated for each of the 400 SAM logic tree sampled branches. In total, this resulted in 4.48 million 1-year-long stochastic catalogues, a number that was deemed sufficient to achieve acceptable convergence for the quantities of interest.

Figure 7 presents the obtained AAL (epistemic) distributions for four of the five loss types that were considered, while Figure 8 shows the obtained PML curves for structural/nonstructural economic loss and fatalities. ERM-CH23 predicts a direct economic AAL of 245 M CHF (or 0.084‰ of the total value) from structural/nonstructural components, plus another 28 M CHF (or 0.033‰ of the total value) from contents. This annual economic loss amounts to about 0.03-0.04% of Switzerland's gross domestic product (GDP). The AAL for fatalities, injuries and displaced population is estimated equal to 7.6, 59.5, and 1079.7, respectively. Structural/nonstructural losses of around 10 billion CHF and about 300 fatalities are expected to be exceeded every 200 years on average. Likewise, for a 1000 year return period of exceedance the loss estimates are assessed at around 37 billion CHF and close to 1700 fatalities.
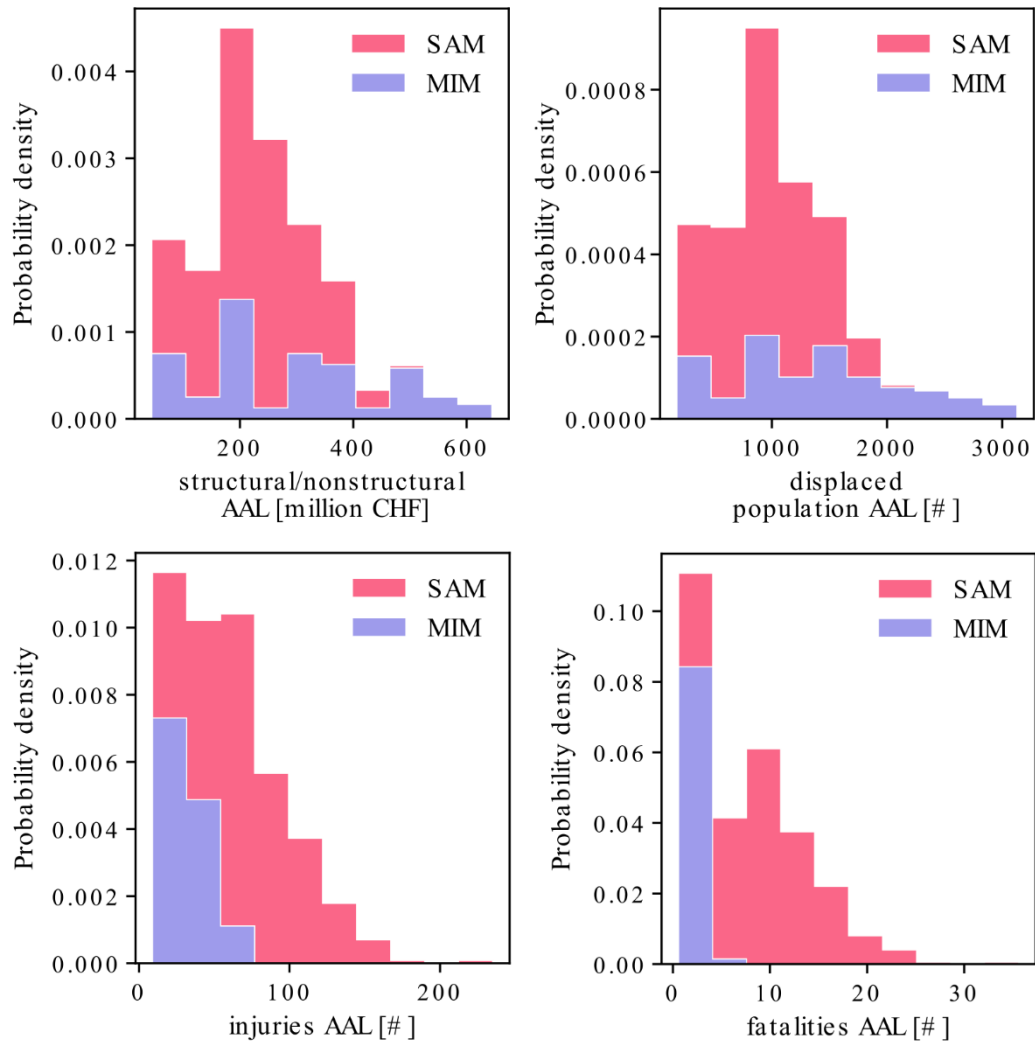
Figure 7. Average annual loss (AAL) epistemic distributions for four loss types. The contributions of the MIM and SAM models are stacked, i.e. at each x-axis bin, the relative heights of the SAM and MIM bars indicate the contribution of the two models at the particular loss value.
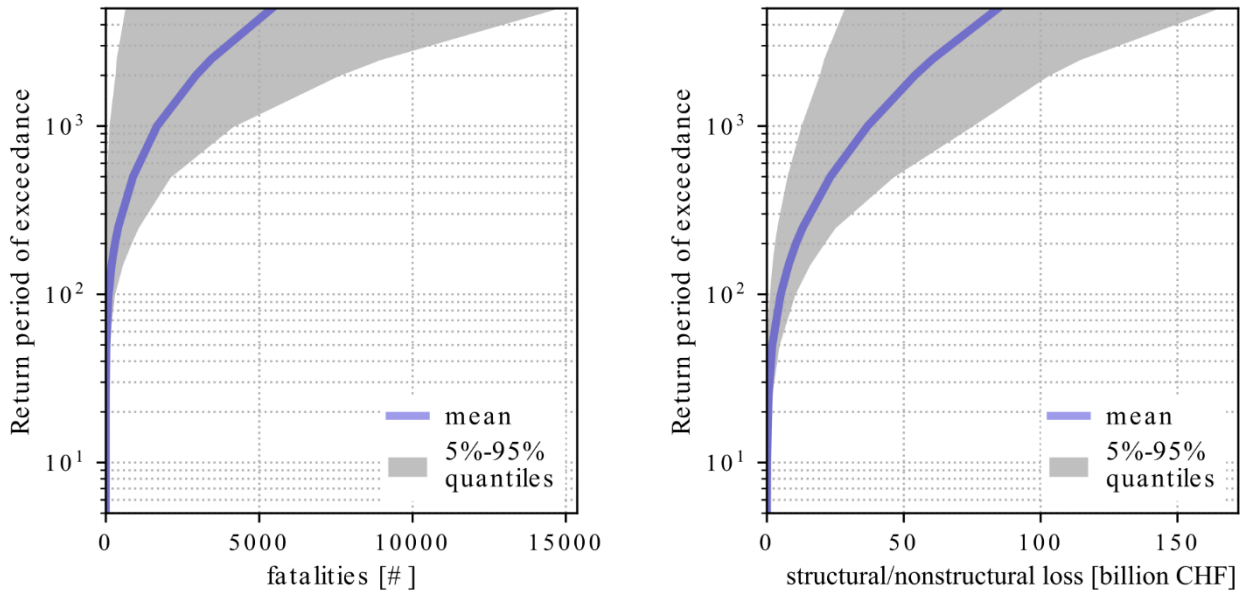
Figure 8. Probable maximum loss curves for fatalities (left) and structural/nonstructural economic loss (right).

320

Of course, as shown in both Figure 7 and Figure 8, there is non-negligible dispersion around the mean estimates reported above, which reflects the large uncertainties in many parts of the model. The main driver of the epistemic uncertainty is the modelling of ground shaking as indicated by the tornado diagrams (Porter et al., 2002) in Figure 9, an observation that is in line with previous studies (e.g. Field et al., 2020). For structural/non-structural AAL, the choice of IPE/GMM leads to a ~5-

325   fold difference, whereas for fatality AAL the difference is ~4-fold for IPEs and 35-fold for GMMs. Important differences are also observed between the two submodels, MIM and SAM, especially for fatalities, as also seen in Figure 7. These large differences in estimated fatalities are attributed to a combination of factors. Fatalities are primarily driven by structural collapses, therefore differences at the least well constrained parts of ground motion and fragility models (i.e. ground motion and intensity amplitudes at short source-to-site distances, collapse fragility functions) manifest in divergent estimates, which

330   reflect the large uncertainty in the estimation of human losses. Lastly, the building mapping scheme and site amplification uncertainties explain a smaller part of the total uncertainty around the country-wide AAL. That said, note that even the latter two sources of epistemic uncertainty might lead to significant differences at local scales (see Wiemer et al., 2023), making their inclusion in the model very important.
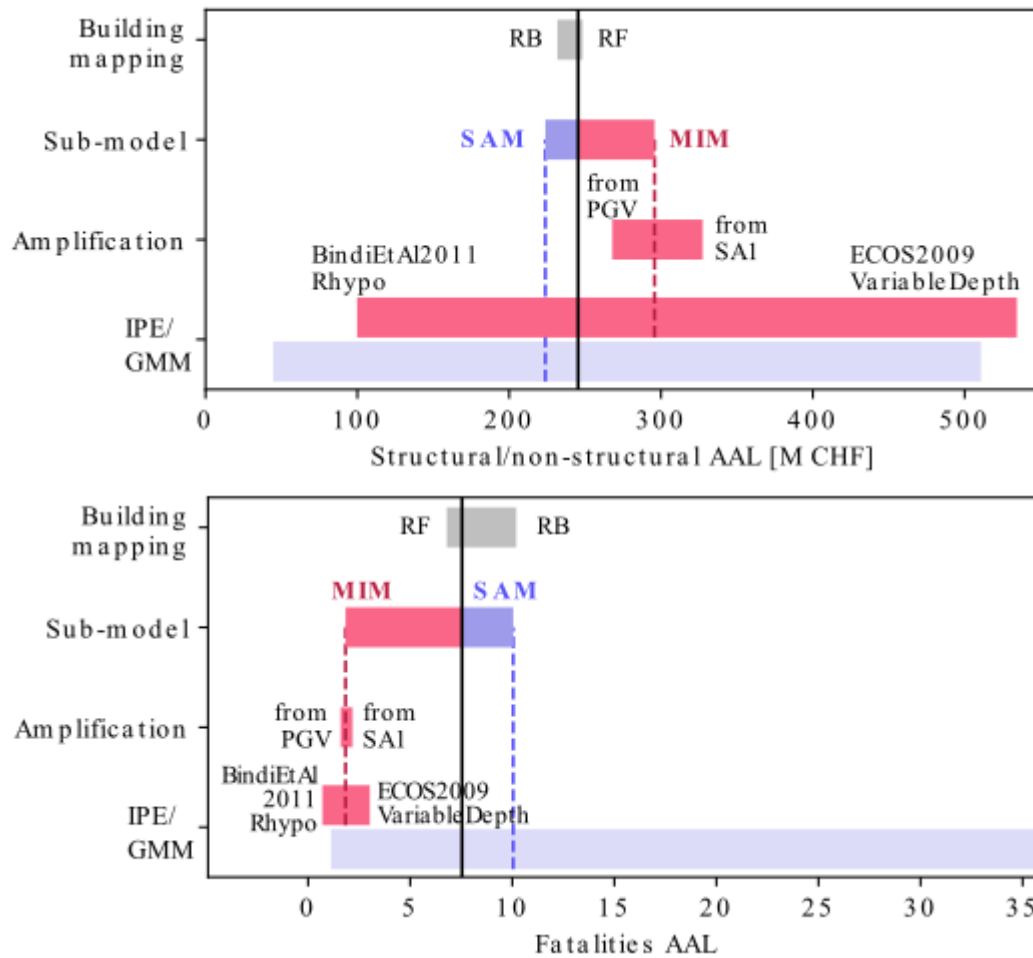
Figure 9. Epistemic ~~variable~~ uncertainty tornado diagrams for structural/non-structural (top) and fatality (bottom) AAL. The bars for each branching level show the minimum and maximum AAL estimate obtained by varying only the input at that level (e.g. only the amplification branch) while keeping the rest of the logic tree unchanged.~~if only the most extreme branches were used at each level, while the remaining logic tree remained the same~~. The MIM and SAM specific bars refer to estimates of those sub-models rather than of the entire model. Finally, in the case of GMMs, since enumeration is not possible and 400 branches are sampled, the bars simply refer to the minimum and maximum values obtained across these 400 samples.

Across the country, the highest AAL estimates are naturally found in areas that combine high concentration of exposure with elevated seismic hazard. The first panel in Figure 10 shows the breakdown of structural/nonstructural AAL across the Swiss cantons. Overall, populous cantons such as those of Bern (BE), Zurich (ZH), and Vaud (VD) feature some of the highest AAL estimates (largely) due their large building stock. High AAL estimates are also found for cantons such as Basel (BS) and Valais (VS) that combine higher seismic hazard with decently sized exposure. The second panel of Figure 10 presents the spatial distribution of AAL ratio (AALR) by municipality. Here, we see that when losses are normalized by the total replacement cost, the spatial pattern tracks the pattern of seismic hazard (on soil conditions). Indeed, municipalities in the south-western

335

340

345

canton of Valais stand out, as a result of the increased seismicity rates and high site amplification along the valley, where most cities are located.
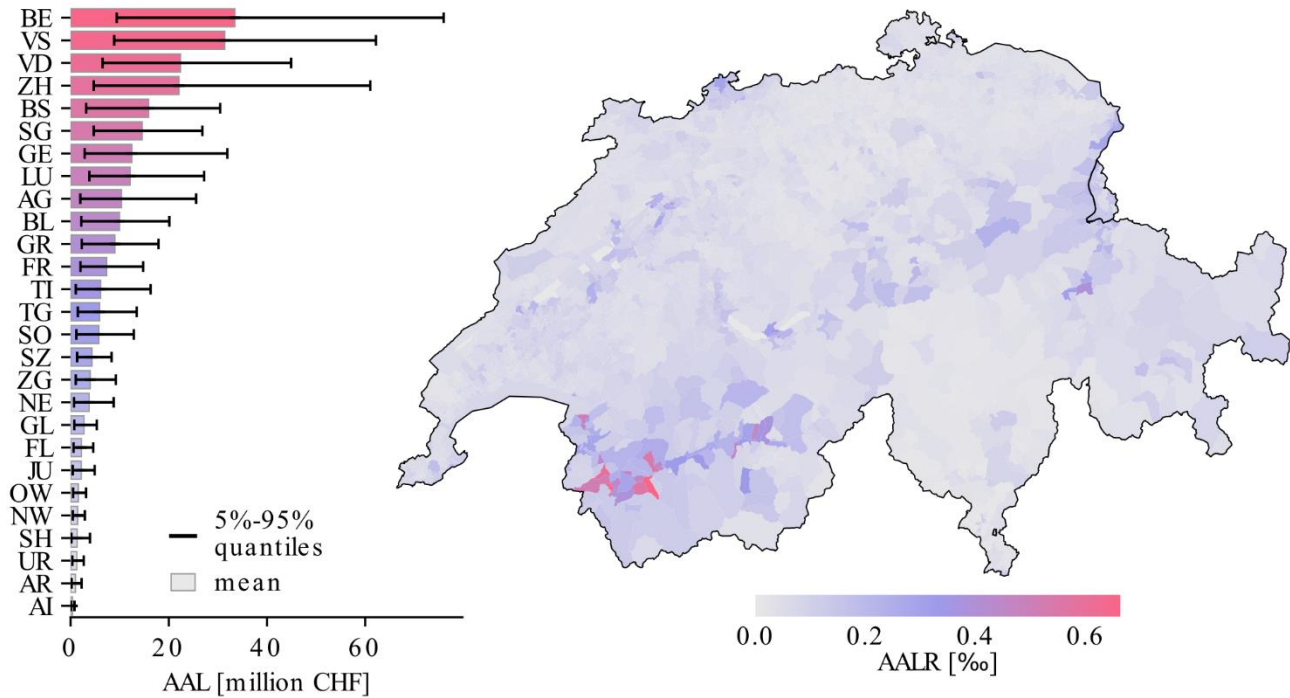
Figure 10. Structural/nonstructural AAL by canton (left) and AALR by municipality (right)

Figure 11 compares the structural/nonstructural AAL and AALR obtained for different structural typologies. Overall, M1, M3 and M5 typologies, and especially the mid- and high-rise variations, display the largest AALR. However, the largest contributions towards the total country-wide AAL come from the M3_L, M6_L, M3_M and RCW_L classes. This reflects the combination of their frequency within the exposure model and their relative vulnerability.
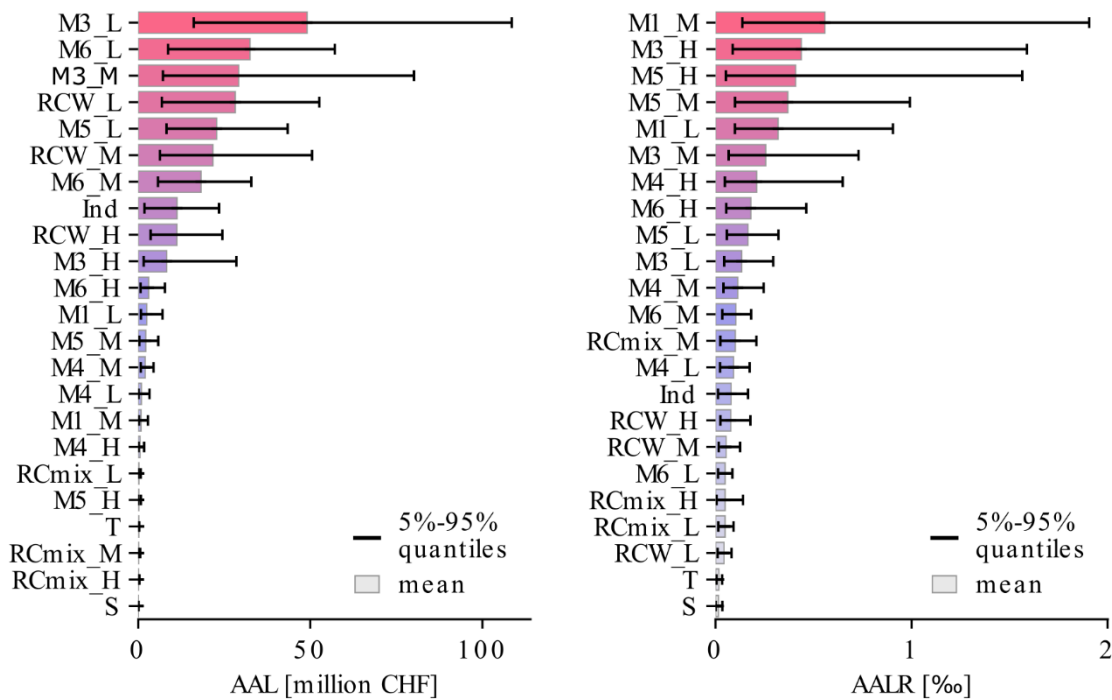
Figure 11. Structural/nonstructural AAL (left) and AALR (right) by building typology

5 Discussion

The risk view provided by ERM-CH23 offers a basis for earthquake risk management in Switzerland. That said, there are several dimensions of earthquake risk that ERM-CH23 does not cover in its first iteration. Earthquake losses quantified by the model refer, solely, to loss induced to the building stock by direct physical damage caused by ground shaking. Damage to infrastructure services (water, wastewater, energy, telecommunications, transport, etc.) and secondary effects (Daniell et al., 2017) from soil liquefaction, landslides, lake tsunamis, fire following or triggered technological accidents (Na-Tech) are not modelled. Indirect losses, such as those incurred from business interruption are also not estimated, nor are possible demand surge effects due to scarcity of human and material resources and overall disruption of supply chains.

An important hurdle for modelling risk in areas of low and moderate seismicity is the lack of historical data for model calibration and validation. Lacking past damage observations, validation was based on subjecting the individual components, as well as the overall model, to sanity checks and verification exercises. Damage and loss analyses were carried out for a wide range of earthquake scenarios. The spatial pattern of modelled ground motion and damage from small and large earthquakes was qualitatively assessed and contrasted with other models and observations. The relative vulnerability of the considered building classes was also subjected to scrutiny and it was made sure that it reasonably matches engineering expectations. The

development of the model was followed by a panel of independent experts to ensure that it conforms with current state-of-the-art practices, while the finalized model was presented and received peer-review by a second independent expert panel.

Lastly, comparisons with the recent European Seismic Risk Model (ESRM20; Crowley et al., 2021) model, GEM's 2018 Global Risk Model (Silva et al., 2020c), and the 2015 Global Assessment Report (GAR; Cardona et al., 2014) were conducted to place our results among other estimates and understand the reasons for any deviations. Table 4Table 4 compares AAL estimates between the aforementioned models and ERM-CH23, while Figure 12 contrasts their reported PML curves. GAR15, which is the least detailed model of the four, yields the higher loss estimates with a frequency that seems generally on the high-side. ESRM20 and GEM18 on the other hand predict significantly lower losses compared to ERM-CH23. The difference is smaller when looking at the AALR, which indicates a large difference in the total exposure value considered between the models. This was found to indeed be the case, as illustrated in Figure 13. This difference can explain about half the discrepancy with ESRM20 and the most part of the discrepancy with GEM18. ERM-CH23 uses a near-complete database of building objects within the country, whereas the assessment of replacement costs is informed by cantonal insurance sources, which lends credibility to the modelling.

Table 4. Comparison of ERM-CH23 AAL estimates with other models

		ERM-CH23	ESRM20	GEM18	GAR15
Structural/Non-structural loss	AAL	245 M CHF	55 M EUR	100 M USD	785 M USD
	AALR [‰]	0.084	0.043	0.07	
Fatalities	AAL	7.6	2		
	AALR [‰]	0.00099	0.0002		
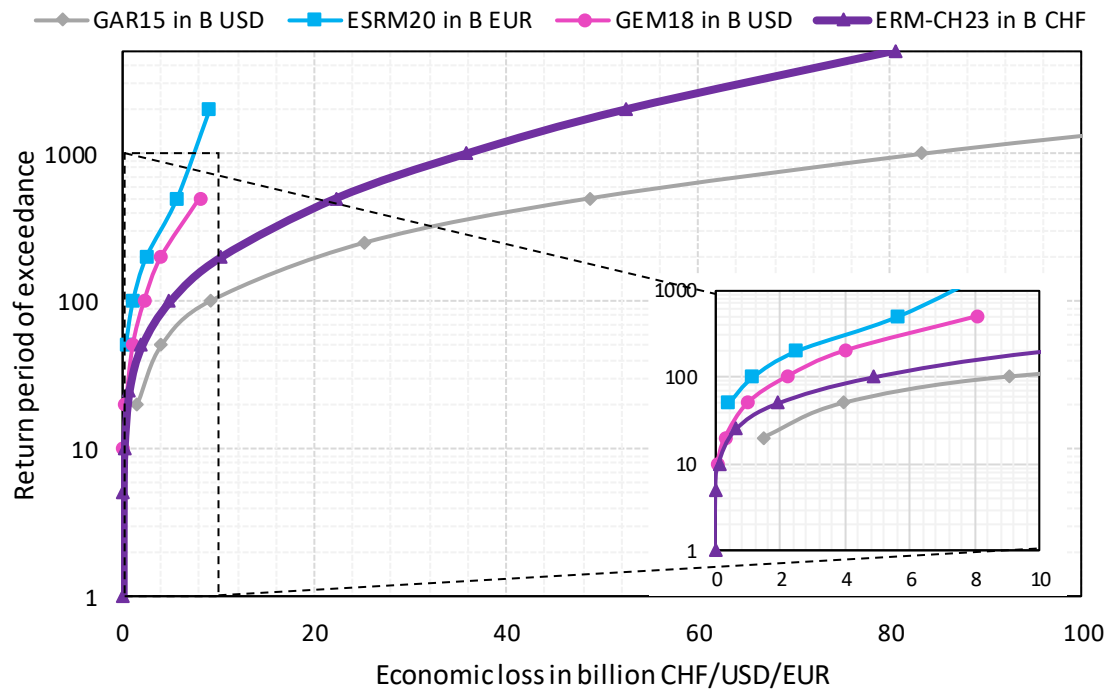
390 **Figure 12. Comparison of structural/nonstructural PML with other models**

A second observation noteworthy is the increased granularity of the site amplification modelling in ERM-CH23. Comparisons with ESRM20 indicated a higher range of site amplification factors in ERM-CH23. This meant higher site amplification in several areas with soft soil deposits (usually around lakes and rivers, where many cities and settlements are located) and lower in mountainous areas with scarce exposure (Figure 13~~13~~). This can explain further differences between ESRM20 and ERM-CH23. Of course, pinpointing the exact factors behind model differences is challenging, since all these models employ very different ground motion, exposure and vulnerability components.
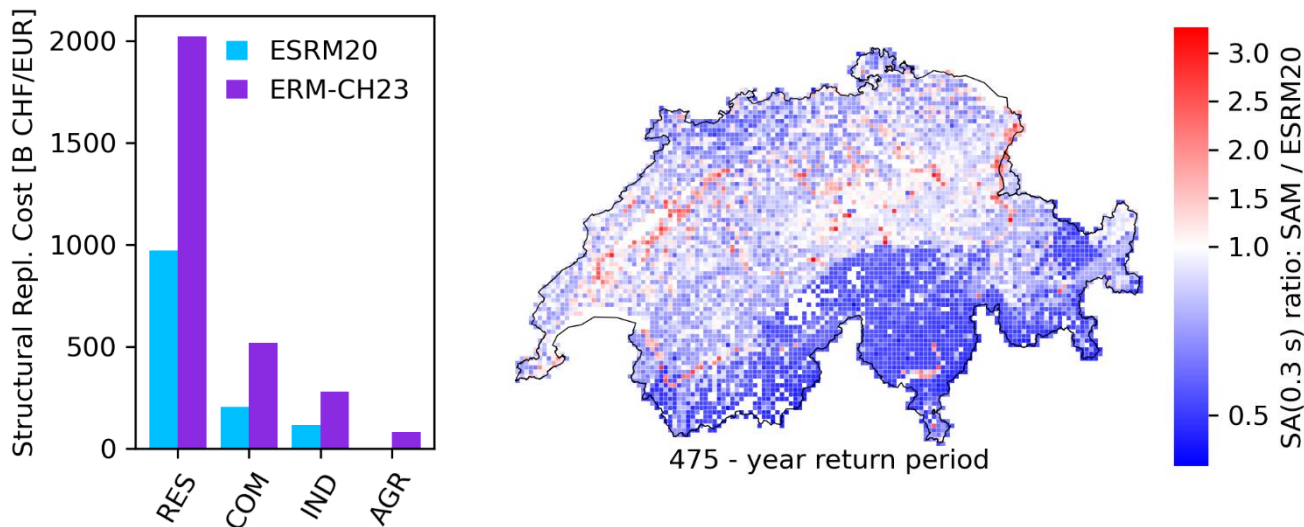
Figure 13. Comparison of total structural replacement cost between ESRM20 and ERM-CH23 (left); Ratio of 475-year SA (0.3 s) values on soil predicted by the SAM component of ERM-CH23 and ESRM20 across Switzerland.

400

6 Communication products and user testing

A dedicated communication concept was needed to bring the insights of the first publicly available earthquake risk model to our different target audiences (Bentele and Nothhaft, 2007). This communication concept consisted of (Wiemer et al., 2023): i) a SWOT (Strengths, Weaknesses, Opportunities, and Threats) analysis to identify the strengths, weaknesses, opportunities,

405   and threats; ii) a definition of the target audiences; iii) a list of the communication goals and key messages; iv) a description of the communication products; v) a planning of the (release) events; and vi) a strategy for the user testing.

Based on the target audiences' needs we developed various products. Some of them support decision-making for earthquake preparedness and response (e.g., scenarios and rapid impact assessments), and others inform about the seismic risk model and

410   its results (e.g., flyer, poster, explainer video, technical report). A key product is the earthquake risk map which depicts an index that combines the expected number of fatalities with the estimated financial losses due to building damage (Figure ~~13~~14). Further, we developed an earthquake risk tool which allows interested people to determine by approximation their personal earthquake risk. The assessment of the personal earthquake risk is based on three factors at the indicated location: the earthquake hazard, the local amplification, the vulnerability of a building depending on the number of storeys and construction

415   period. All products are available on the SED website in the three national languages of Switzerland and in English (see seismo.ethz.ch).
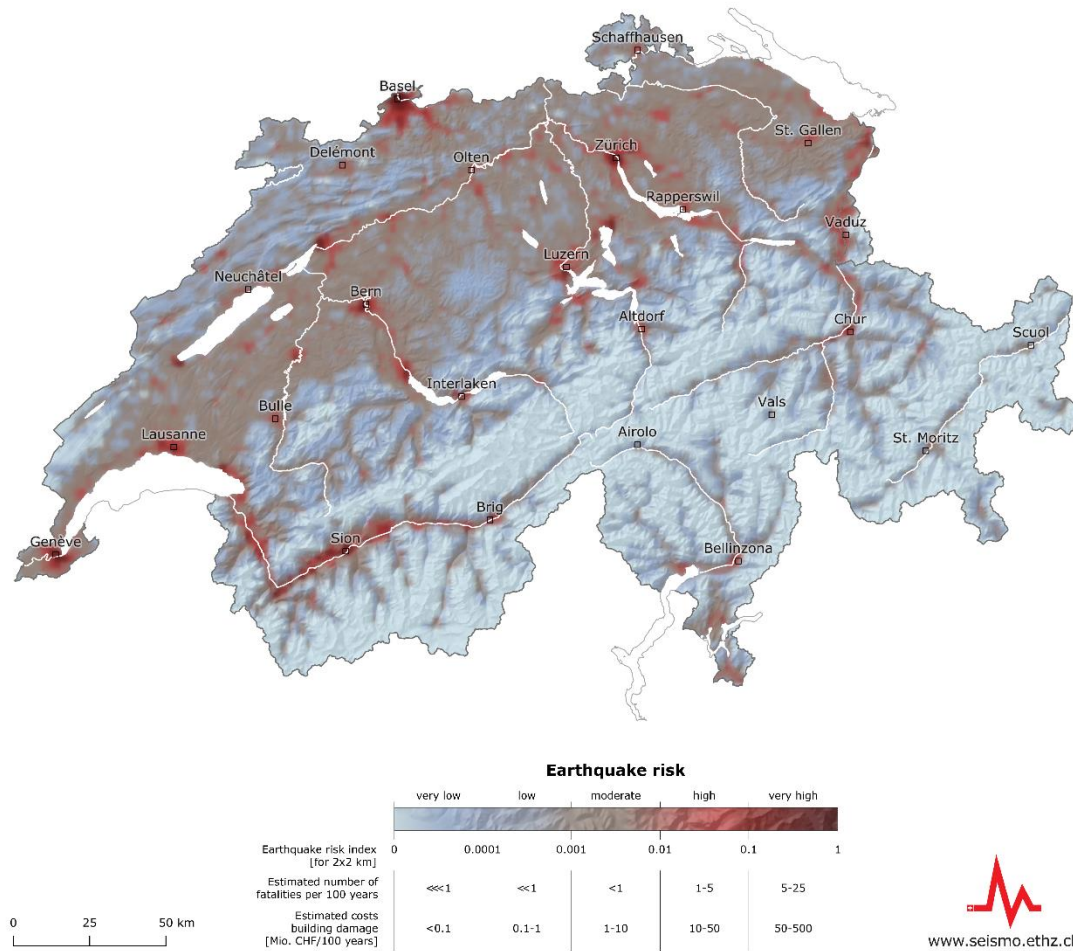
Figure 1~~3~~4. The earthquake risk map of Switzerland

420

To design these user-centered products, testing was indispensable (Dallo et al., 2022; Marti et al., 2019). We thus followed a transdisciplinary approach since we – an interdisciplinary group consisting of model developers, IT specialists, and communication experts – co-developed the products and tested them with the target audiences. We first conducted interviews with international experts to learn from best practices and already operational seismic risk services (e.g. Pager; Dryhurst et al.,

425 2021). Second, we organised workshops with professional stakeholders (e.g., cantonal authorities, civil protection) to assess their information and application needs, and to further develop the prototypes based on their feedback (Marti et al., 2023). Third, we conducted two public surveys to evaluate which rapid impact assessments, scenarios, and risk maps are correctly interpreted, perceived as useful, and preferred (Dallo et al., 2023; Marti et al., 2023; Dallo et al., 2024a). For the product design, we further benefitted from our experiences of the release of the first European Seismic Risk Model (ESRM2020; Dallo

430 et al., ~~in preparation~~2024b).

7 Conclusion

This study summarized the development of the first Earthquake Risk Model of Switzerland, ERM-CH23, and provided key results. ERM-CH23 represents an important milestone in advancing the understanding of earthquake risk in the country. Estimates of the size and spatial pattern of earthquake risk in Switzerland was previously lacking from the public domain and inferences had to be made relying on solely hazard information. By filling this gap, our hope is that ERM-CH23 will encourage evidence-based decision-making by public authorities and other stakeholders, in efforts towards risk mitigation and disaster resilience. Further downstream products of the ERM-CH23 project are also expected to underpin disaster preparedness and response. A rapid impact assessment service has also been devised, using the ERM-CH23 framework to produce near real-time estimates of damage and loss after the occurrence of earthquakes. This system will use ground motion footprints updated with station recordings, as implemented in the Swiss ShakeMap service (Cauzzi et al., 2015). In the future, the National Earthquake Risk Model of Switzerland should be periodically updated and improved, incorporating the latest science and datasets. Extensions to cover secondary perils, indirect losses and infrastructure should also be planned to enable a holistic view or earthquake risk.

8 Author contribution

Conceptualization: ANP, DF, MM, LD, BD, PL, SW; Data curation: ANP, FP, BD, LD, AK; Formal analysis: ANP, FP, PB, DF, OO, LD, BD, AK,; Funding acquisition: SW, DF, PR, FH, BD; Methodology: ANP, FP, PB, DF, MM, ID, OO, EF, CC, AK, PL, LD, BD; Project administration: PR, DF, NV, MM, FH, SW; Resources: SW, MM, ID, PR, NS, PK, LD; Software: ANP, CC, NS, PK, LD; Supervision: SW, ANP, DF, PB, PR, LD, PL; Validation: ANP, DF, CC, PR, LD, BD ; Visualization: ANP; Writing: ANP, NV, ID; Writing – review & editing: ANP, FP, PB, DF, CC, PR

9 Competing interests

The authors declare that they have no conflict of interest.

10 Acknowledgements

The development of the ERM-CH23 model was co-funded by ETH Zurich (contract ID 19203), the Federal Office for Civil Protection (FOCP; contract no. 353007634), and the Federal Office for the Environment (FOEN; contract no. 16.0115.PJ / Q114-1464). The development of communication products also benefitted from partial funding from European Union's Horizon 2020 research and innovation program under grant agreement Real-time earthquake rIsk reduction for a reSilient Europe (RISE) project (http://www.rise-eu.org) No. 821115.

11 References

460 Akkar, S. and Bommer, J. J.: Empirical equations for the prediction of PGA, PGV, and spectral accelerations in Europe, the mediterranean region, and the Middle East, Seismol. Res. Lett., 81, 195–206, https://doi.org/10.1785/gssrl.81.2.195, 2010.

Baumont, D., Manchuel, K., Traversa, P., Durouchoux, C., Nayman, E., and Ameri, G.: Intensity predictive attenuation models calibrated in Mw for metropolitan France, Bull. Earthq. Eng., 16, 2285–2310, https://doi.org/10.1007/s10518-018-0344-6, 2018.

465 Bentele, G. and Nothhaft, H.: Konzeption von Kommunikationsprogrammen, in: Handbuch Unternehmenskommunikation, Gabler Verlag, Wiesbaden, 357–380, https://doi.org/10.1007/978-3-8349-9164-5_18, 2007.

Bergamo, P., Fäh, D., Panzera, F., Cauzzi, C.V., Glueer, F., Perron, V., and Wiemer, S.: A site amplification model for Switzerland based on site condition indicators and incorporating local response as measured at seismic stations. Bull Earthquake Eng 21, 5831–5865 (2023). https://doi.org/10.1007/s10518-023-01766-z Submitted to Bull. Earthq. Eng.

470 Bernardini, A., Lagomarsino, S., Mannella, A., Martinelli, A., Milano, L., Parodi, S., and Troffaes, M.: Forecasting seismic damage scenarios of residential buildings from rough inventories: a case study in the Abruzzo Region (Italy), Proc. Inst. Mech. Eng., 4, 279–296, https://doi.org/10.1243/1748006XJRR305, 2010.

Bindi, D., Parolai, S., Oth, A., Abdrakhmatov, K., Muraliev, A., and Zschau, J.: Intensity prediction equations for Central Asia, Geophys. J. Int., 187, 327–337, https://doi.org/10.1111/j.1365-246X.2011.05142.x, 2011.

475 Bommer, J. J. and Crowley, H.: The Purpose and Definition of the Minimum Magnitude Limit in PSHA Calculations, Seismol. Res. Lett., 88, 1097–1106, https://doi.org/10.1785/0220170015, 2017.

Cardona, O. D., Ordaz, M. G., Mora, M. G., Salgado-Gálvez, M. A., Bernal, G. A., Zuloaga-Romero, D., Marulanda Fraume, M. C., Yamín, L., and González, D.: Global risk assessment: A fully probabilistic seismic and tropical cyclone wind risk assessment, Int. J. Disaster Risk Reduct., 10, 461–476, https://doi.org/10.1016/j.ijdrr.2014.05.006, 2014.

480 Cauzzi, C. and Faccioli, E.: Broadband (0.05 to 20 s) prediction of displacement response spectra based on worldwide digital records, J. Seismol., 12, 453–475, https://doi.org/10.1007/s10950-008-9098-y, 2008.

Cauzzi, C., Edwards, B., Fäh, D., Clinton, J., Wiemer, S., Kästli, P., Cua, G., and Giardini, D.: New predictive equations and site amplification estimates for the next-generation Swiss ShakeMaps, Geophys. J. Int., 200, 421–438, https://doi.org/10.1093/gji/ggu404, 2015.

485 Chiou, B.-J. and Youngs, R. R.: An NGA Model for the Average Horizontal Component of Peak Ground Motion and Response Spectra, Earthq. Spectra, 24, 173–215, https://doi.org/10.1193/1.2894832, 2008.

Crowley, H., Dabbeek, J., Despotaki, V., Rodrigues, D., Martins, L., Silva, V., Romao, X., Pereira, N., Weatherill, G., and Danciu, L.: European Seismic Risk Model (ESRM20), https://doi.org/10.7414/EUC-EFEHR-TR002-ESRM20, 2021.

Dallo, I., Stauffacher, M., and Marti, M.: Actionable and understandable? Evidence-based recommendations for the design of
490 (multi-)hazard warning messages, Int. J. Disaster Risk Reduct., 74, https://doi.org/10.1016/j.ijdrr.2022.102917, 2022.

Dallo, I., Schnegg, L. N., and Marti, M.: The design of user-centred seismic risk maps – the Swiss case, in: EGU General Assembly 2023, https://doi.org/10.5194/egusphere-egu23-3241, 2023.

Dallo, I., Marti, M., Valenzuela, N., Crowley, H., Dabbeek, J., Danciu, L., Zaugg, S., Cotton, F., Giardini, D., Pinho, R., Schneider, J. F., Beauval, C., Correia, A. A., Ktenidou, O. J., Mäntyniemi, P., Pagani, M., Silva, V., Weatherill, G., and Wiemer, S.: The communication strategy for the release of the first European Seismic Risk Model and the updated European Seismic Hazard Model, Nat. Hazards Earth Syst. Sci., 24, 291–307, https://doi.org/10.5194/nhess-24-291-2024, 2024., in preparation.

Dallo, I., Schnegg, L. N., and Marti, M, Fulda, D., Papadopoulos, A.N., Roth, P., Danciu, L.,Valenzuela, N., Wenk, S. R., Bergamo, P., Haslinger, F., Fäh, D., Kästli, P., and Wiemer, S.: Designing understandable, action-oriented, and well-perceived earthquake risk maps—The Swiss case study, Front. Commun. 8:1306104, doi: 10.3389/fcomm.2023.1306104, 2024.

Daniell, J. E., Schaefer, A. M., and Wenzel, F.: Losses associated with secondary effects in earthquakes, Front. Built Environ., 3, 1–14, https://doi.org/10.3389/fbuil.2017.00030, 2017.

Diana, L., Thiriot, J., Reuland, Y., and Lestuzzi, P.: Application of Association Rules to Determine Building Typological Classes for Seismic Damage Predictions at Regional Scale: The Case Study of Basel, Front. Built Environ., 5, https://doi.org/10.3389/fbuil.2019.00051, 2019.

Dolce, M., Prota, A., Borzi, B., da Porto, F., Lagomarsino, S., Magenes, G., Moroni, C., Penna, A., Polese, M., Speranza, E., Verderame, G. M., and Zuccaro, G.: Seismic risk assessment of residential buildings in Italy, Springer Netherlands, 2999–3032 pp., https://doi.org/10.1007/s10518-020-01009-5, 2021.

Dryhurst, S., Luoni, G., Dallo, I., Freeman, A. L. J., and Marti, M.: Designing & implementing the seismic portion of dynamic risk communication for long-term risks, variable short-term risks, early warnings (Society: Data Gathering and Information Sharing with the Public and Policy-Makers) [Deliverable]. European Horizon-2020 project RISE. http://static.seismo.ethz.ch/rise/deliverables/Deliverable_5.3.pdf#page=56&zoom=100, 92, 948, 2021.

Edwards, B. and Fäh, D.: A Stochastic ground-motion model for Switzerland, Bull. Seismol. Soc. Am., 103, 78–98, https://doi.org/10.1785/0120110331, 2013.

Edwards, B., Michel, C., Poggi, V., and Fäh, D.: Determination of site amplification from regional seismicity: Application to the Swiss national seismic networks, Seismol. Res. Lett., 84, 611–621, https://doi.org/10.1785/0220120176, 2013.

Edwards, B., Cauzzi, C., Danciu, L., and Fäh, D.: Region-Specific Assessment, Adjustment, and Weighting of Ground-Motion Prediction Models: Application to the 2015 Swiss Seismic-Hazard Maps, Bull. Seismol. Soc. Am., 106, 1840–1857, https://doi.org/10.1785/0120150367, 2016.

Faenza, L. and Michelini, A.: Regression analysis of MCS intensity and ground motion parameters in Italy and its application in ShakeMap, Geophys. J. Int., 180, 1138–1152, https://doi.org/10.1111/j.1365-246X.2009.04467.x, 2010.

Faenza, L. and Michelini, A.: Regression analysis of MCS intensity and ground motion spectral accelerations (SAs) in Italy, Geophys. J. Int., 186, 1415–1430, https://doi.org/10.1111/j.1365-246X.2011.05125.x, 2011.

Fäh, D., Gisler, M., Jaggi, B., Kästli, P., Lutz, T., Masciadri, V., Matt, C., Mayer-Rosa, D., Rippmann, D., Schwarz-Zanetti, G., Tauber, J., and Wenk, T.: The 1356 Basel earthquake: An interdisciplinary revision, Geophys. J. Int., 178, 351–374, https://doi.org/10.1111/j.1365-246X.2009.04130.x, 2009.

Fäh, D., Giardini, D., Kästli, P., Deichmann, N., Gisler, M., Schwarz-Zanetti, G., Alvarez-Rubio, S., Sellami, S., Edwards, B., and Allmann, B.: ECOS-09 earthquake catalogue of Switzerland release 2011 report and database. Public catalogue, 17. 4. 2011., 1–42 pp., 2011.

Federal Emergency Management Agency (FEMA): Seismic Performance Assessment of Buildings, Washington, D.C., https://doi.org/10.4231/D3ZW18S8N, 2018.

FEMA: Multi-hazard Loss Estimation Methodology Earthquake Model Hazus®-MH MR5: Technical Manual, Washington, D.C., 2010.

Field, E. H., Milner, K. R., and Porter, K. A.: Assessing the value of removing earthquake-hazard-related epistemic uncertainties, exemplified using average annual loss in California, Earthq. Spectra, 36, 1912–1929, https://doi.org/10.1177/8755293020926185, 2020.

FOCP: National risk analysis report. Disasters and Emergencies in Switzerland 2020, Bern, 60 pp., 2020.

FOEN: Earthquake Risk Model Switzerland (ERM-CH) – Subproject F, Database of building objects - Deliverable DB4, report. SPG-SPD-0015, 2021.

Fritsche, S. and Fäh, D.: The 1946 magnitude 6.1 earthquake in the Valais: site-effects as contributor to the damage, Swiss J. Geosci., 102, 423, https://doi.org/10.1007/s00015-009-1340-2, 2009.

Fritsche, S., Fäh, D., Gisler, M., and Giardini, D.: Reconstructing the damage field of the 1855 earthquake in Switzerland: Historical investigations on a well-documented event, Geophys. J. Int., 166, 719–731, https://doi.org/10.1111/j.1365-246X.2006.02994.x, 2006.

Grünthal, G.: European Macroseismic Scale 1998 (EMS-98), Luxembourg, 1998.

Hengl, T., Heuvelink, G. B. M., and Rossiter, D. G.: About regression-kriging: From equations to case studies, Comput. Geosci., 33, 1301–1315, https://doi.org/10.1016/j.cageo.2007.05.001, 2007.

Hobbs, T. E., Journeay, J. M., Rao, A. S., Kolaj, M., Martins, L., LeSueur, P., Simionato, M., Silva, V., Pagani, M., Johnson, K., Rotheram, D., and Chow, W.: A national seismic risk model for Canada: Methodology and scientific basis, Earthq. Spectra, 875529302311734, https://doi.org/10.1177/87552930231173446, 2023.

Hügli, M., Zischg, A., Keiler, M.: Modellierung von Gebäudeattributen im Rahmen des Projektes Erdbeben- risikomodell Schweiz – dritte Arbeitsphase. Bericht im Auftrag vom Bundesamt für Umwelt. EXT-TR-0017, 2021.

Jaiswal, K. S., Bausch, D., Chen, R., Bouabid, J., and Seligson, H.: Estimating annualized earthquake losses for the conterminous United States, Earthq. Spectra, 31, S221–S243, https://doi.org/10.1193/010915EQS005M, 2015.

Lagomarsino, S. and Giovinazzi, S.: Macroseismic and mechanical models for the vulnerability and damage assessment of current buildings, Bull. Earthq. Eng., 4, 415–443, https://doi.org/10.1007/s10518-006-9024-z, 2006.

Lagomarsino, S., Cattari, S., and Ottonelli, D.: The heuristic vulnerability model: fragility curves for masonry buildings, Bull. Earthq. Eng., 19, 3129–3163, https://doi.org/10.1007/s10518-021-01063-7, 2021.

Lestuzzi, P., Podestà, S., Luchini, C., Garofano, A., Kazantzidou-Firtinidou, D., Bozzano, C., Bischof, P., Haffter, A., and Rouiller, J. D.: Seismic vulnerability assessment at urban scale for two typical Swiss cities using Risk-UE methodology, Nat. Hazards, 84, 249–269, https://doi.org/10.1007/s11069-016-2420-z, 2016.

Lestuzzi, P., Podestà, S., Luchini, C., Garofano, A., Kazantzidou-Firtinidou, D., and Bozzano, C.: Validation and improvement of Risk-UE LM2 capacity curves for URM buildings with stiff floors and RC shear walls buildings, Bull. Earthq. Eng., 15, 1111–1134, https://doi.org/10.1007/s10518-016-9981-9, 2017.

Liu, L. and Pezeshk, S.: An improvement on the estimation of pseudoresponse spectral velocity using RVT method, Bull. Seismol. Soc. Am., 89, 1384–1389, https://doi.org/10.1785/BSSA0890051384, 1999.

MacQueen, J.: Some methods for classification and analysis of multivariate observations, in: Proceedings of the Fifth Berkeley Symposium on Mathematical Statistics and Probability, Volume 1: Statistics, 1967.

Marques, M., Monteiro, R., and Delgado, R.: An improved model for seismic risk assessment in Portugal, Int. J. Disaster Resil. Built Environ., 9, 70–83, https://doi.org/10.1108/IJDRBE-10-2016-0040, 2018.

Marti, M., Stauffacher, M., and Wiemer, S.: Difficulties in explaining complex issues with maps: Evaluating seismic hazard communication - The Swiss case, Nat. Hazards Earth Syst. Sci., 19, 2677–2700, https://doi.org/10.5194/nhess-19-2677-2019, 2019.

Marti, M., Dallo, I., Roth, P., Papadopoulos, A. N., and Zaugg, S.: Illustrating the impact of earthquakes: Evidence-based and user-centered recommendations on how to design earthquake scenarios and rapid impact assessments, Int. J. Disaster Risk Reduct., 90, 103674, https://doi.org/10.1016/j.ijdrr.2023.103674, 2023.

Michel, C., Crowley, H., Hannewald, P., Lestuzzi, P., and Fäh, D.: Deriving fragility functions from bilinearized capacity curves for earthquake scenario modelling using the conditional spectrum, Bull. Earthq. Eng., 1–22, https://doi.org/10.1007/s10518-018-0371-3, 2018.

NCPD: National risk assessment: Overview of the potential major disasters in Italy: seismic, volcanic, tsunami, hydro-geological/hydraulic and extreme weather, droughts and forest fire risks, 2018.

Pagani, M., Monelli, D., Weatherill, G., Danciu, L., Crowley, H., Silva, V., Henshaw, P., Butler, L., Nastasi, M., Panzeri, L., Simionato, M., and Vigano, D.: OpenQuake Engine: An Open Hazard (and Risk) Software for the Global Earthquake Model, Seismol. Res. Lett., 85, 692–702, https://doi.org/10.1785/0220130087, 2014.

Panzera, F., Bergamo, P., and Fäh, D.: Reference soil condition for intensity prediction equations derived from seismological and geophysical data at seismic stations, J. Seismol., 25, 163–179, https://doi.org/10.1007/s10950-020-09962-z, 2021.

Papadopoulos, A.N., Roth, P., and Danciu, L.: Exposure manipulation strategies for optimizing computational efficiency in seismic risk analysis ~~of large building portfolios, in preparation.~~, Bull Earthquake Eng 22, 4779–4795, https://doi.org/10.1007/s10518-024-01929-6, 2024

590   Poggi, V., Edwards, B., and Fah, D.: Derivation of a Reference Shear-Wave Velocity Model from Empirical Site Amplification, Bull. Seismol. Soc. Am., 101, 258–274, https://doi.org/10.1785/0120100060, 2011.

Porter, K. A., Beck, J. L., and Shaikhutdinov, R. V.: Sensitivity of building loss estimates to major uncertain variables, Earthq. Spectra, 18, 719–743, https://doi.org/10.1193/1.1516201, 2002.

Röthlisberger, V., Zischg, A. P., and Keiler, M.: A comparison of building value models for flood risk analysis, Nat. Hazards

595   Earth Syst. Sci., 18, 2431–2453, https://doi.org/10.5194/nhess-18-2431-2018, 2018.

Salgado-Gálvez, M. A., Cardona, O. D., Carreño, M. L., and Barbat, A. H.: Probabilistic seismic hazard and risk assessment in Spain: national and local level case studies, 1–215 pp., 2015.

Silva, V., Amo-Oduro, D., Calderon, A., Costa, C., Dabbeek, J., Despotaki, V., Martins, L., Pagani, M., Rao, A., Simionato, M., Viganò, D., Yepes-Estrada, C., Acevedo, A., Crowley, H., Horspool, N., Jaiswal, K., Journeay, M., and Pittore, M.:

600   Development of a global seismic risk model, Earthq. Spectra, 36, 372–394, https://doi.org/10.1177/8755293019899953, 2020a.

Silva, V., Amo-Oduro, D., Calderon, A., Costa, C., Dabbeek, J., Despotaki, V., Martins, L., Pagani, M., Rao, A., Simionato, M., Viganò, D., Yepes-Estrada, C., Acevedo, A., Crowley, H., Horspool, N., Jaiswal, K., Journeay, M., and Pittore, M.: Development of a global seismic risk model, Earthq. Spectra, 875529301989995, https://doi.org/10.1177/8755293019899953,

605   2020b.

Spence, R., So, E., Ameri, G., Akinci, A., Cocco, M., Cultrera, G., Franceschina, G., Pacor, F., Pessina, V., Lombardi, A. M., Zonno, G., Carvalho, A., Campos Costa, A., Coelho, E., Pitilakis, K., Anastasiadis, A., Kakderi, K., Alexoudi, M., Ansal, A., Erdic, M., Tonuk, G., and Demircioglu, M.: Earthquake Disaster Scenario Prediction and Loss Modelling for Urban Areas, IUSS Press, Pavia, 2007.

610   Tin Kam Ho: The random subspace method for constructing decision forests, IEEE Trans. Pattern Anal. Mach. Intell., 20, 832–844, https://doi.org/10.1109/34.709601, 1998.

Tyagunov, S., Grünthal, G., Wahlström, R., Stempniewski, L., and Zschau, J.: Seismic risk mapping for Germany, Nat. Hazards Earth Syst. Sci., 6, 573–586, https://doi.org/10.5194/nhess-6-573-2006, 2006.

Wiemer, S., Giardini, D., Fäh, D., Deichmann, N., and Sellami, S.: Probabilistic seismic hazard assessment of Switzerland:

615   Best estimates and uncertainties, J. Seismol., 13, 449–478, https://doi.org/10.1007/s10950-008-9138-7, 2009.

Wiemer, S., Danciu, L., Edwards, B., Marti, M., Fäh, D., Hiemer, S., Wössner, J., Cauzzi, C., Kästli, P., and Kremer, K.: Seismic Hazard Model 2015 for Switzerland (SUIhaz2015), Swiss Seismological Service (SED) at ETH Zurich, 164 pp., 2016.

Wiemer, S., Papadopoulos, A., Roth, P., Danciu, L., Bergamo, P., Fäh, D., Duvernay, B., Khodaverdian, A., Lestuzzi, P., Odabaşı, O., Fagà, E., Bazzurro, P., Cauzzi, C., Hammer, C., Panzera, F., Perron, V., Marti, M., Valenzuela, N., Dallo, I.,

620   Zaugg, S., Fulda, D., Kästli, P., Schmid, N., and Haslinger, F.: Earthquake Risk Model of Switzerland ERM-CH23, Swiss Seismological Service (SED), https://doi.org/10.12686/a20, 2023.

Woessner, J., Danciu, L., Giardini, D., Crowley, H., Cotton, F., Grünthal, G., Valensise, G., Arvidsson, R., Basili, R., Demircioglu, M. B., Hiemer, S., Meletti, C., Musson, R. W., Rovida, A. N., Sesetyan, K., and Stucchi, M.: The 2013 European

Seismic Hazard Model: key components and results, Bull. Earthq. Eng., 13, 3553–3596, https://doi.org/10.1007/s10518-015-9795-1, 2015.

Zhao, J. X.: Attenuation Relations of Strong Ground Motion in Japan Using Site Classification Based on Predominant Period, Bull. Seismol. Soc. Am., 96, 898–913, https://doi.org/10.1785/0120050122, 2006.

630